

Adaptive EGF expression sensitizes pancreatic cancer cells to ionizing radiation through activation of the cyclin D1/P53/PARP pathway

XIAOXING LIU^{1*}, HAIYAN CHEN^{1*}, YANLI HOU¹, XIUMEI MA¹, MING YE¹, RENHUA HUANG¹, BIN HU¹, HONGBIN CAO¹, LEI XU¹, MENGYAO LIU², LINFENG LI², JIANXIN GAO^{2,3} and YONGRUI BAI¹

¹Department of Radiation Oncology; ²Laboratory of Tumorigenesis and Immunity, Clinical Stem Cell Research Center;

³State Key Laboratory of Oncogene and Related Genes, Renji Hospital, Shanghai Jiao Tong University School of Medicine, Shanghai 200127, P.R. China

Received September 24, 2018; Accepted February 2, 2019

DOI: 10.3892/ijo.2019.4719

Abstract. It is well-known that the activation status of the P53, signal transducer and activator of transcription (Stat)3 and nuclear factor (NF)- κ B signaling pathways determines the radiosensitivity of cancer cells. However, the function of these pathways in radiosensitive vs radioresistant cancer cells remains elusive. The present study demonstrated that adaptive expression of epidermal growth factor (EGF) following exposure to ionizing radiation (IR) may induce radiosensitization of pancreatic cancer (PC) cells through induction of the cyclin D1/P53/poly(ADP-ribose) polymerase pathway. By contrast, adaptively expressed interleukin (IL)-6 and insulin-like growth factor (IGF)-1 may promote radioresistance of PC cells, likely through activation of the Stat3 and NF- κ B pathways. In addition, cyclin D1 and survivin, which are specifically expressed in the G1/S and G2/M phase of the cell cycle, respectively, are mutually exclusive in radiosensitive and radioresistant PC cells, while Bcl-2 and Bcl-xL expression does not differ between radiosensitive and radioresistant PC cells. Therefore, adaptively expressed EGF and IL-6/IGF-1 may alter these pathways to promote the radiosensitivity of PC cancers. The findings of the present study highlight potential

markers for the evaluation of radiosensitivity and enable the development of effective regimens for cancer radiotherapy.

Introduction

Pancreatic ductal adenocarcinoma (PDAC) is the fourth leading cause of cancer-related mortality worldwide, although its incidence is lower compared with that of other types (1). In addition to its aggressive nature, the late onset of symptoms, failure to respond to systematic therapy, and its radio and chemoresistance, contribute to a 5-year survival rate of only 5% among pancreatic cancer (PC) patients (2). In addition to surgery, radiotherapy is a standard treatment used for PDAC. However, PDAC cells inevitably develop resistance to radiotherapy. Although extensive investigations have been performed on the mechanisms underlying the radioresistance of cancers and the multiple signaling pathways involved, such as the suppressed P53-mediated apoptosis pathway, the pro-survival cytokine and growth factor-mediated activation of the signal transducer and activator of transcription (Stat)3 and nuclear factor (NF)- κ B pathways, and the impaired DNA damage repair pathway (3,4), the molecular mechanisms that antagonize these pathways have not been fully elucidated in PC cells. Therefore, it is important to explore the mechanisms underlying cancer cell radiosensitivity in order to overcome the radioresistance of PDAC and develop safe, effective regimens.

In the clinical setting, radiotherapy is one of the main adjuvant treatments for cancer and it is frequently applied to patients with PC. Ionizing radiation (IR)-induced apoptosis is considered to be one of the major cell death responses following exposure to irradiation, including X-rays or γ -rays. After irradiation, the DNA damage response cascade is activated, a number of transcription factors, such as P53, are activated, and the DNA repair process is impaired, with subsequent cell cycle arrest, senescence and/or apoptosis (5). While the P53-mediated apoptotic pathway is initiated, radiation-induced cell cycle arrest, failure to repair damaged DNA and inactivation of pro-survival pathways promote cell death (6).

B-cell lymphoma (Bcl)-2 and related family members are key regulators of mitochondrial-related apoptosis (7). This family

Correspondence to: Professor Jianxin Gao, State Key Laboratory of Oncogene and Related Genes, Renji Hospital, Shanghai Jiao Tong University School of Medicine, 160 Pujian Road, Shanghai 200127, P.R. China

E-mail: 15618820486@163.com

Professor Yongrui Bai, Department of Radiation Oncology, Renji Hospital, Shanghai Jiao Tong University School of Medicine, 160 Pujian Road, Shanghai 200127, P.R. China

E-mail: baiyongruiz@163.com

*Contributed equally

Key words: radiosensitivity, epidermal growth factor, cyclin D1, P53, poly(ADP-ribose) polymerase

of proteins is divided into two subfamilies, the pro-apoptotic proteins and anti-apoptotic proteins. The pro-apoptotic Bcl-2 family proteins, such as Bcl-2-associated X (BAX), Bcl-2 homologous antagonist/killer (BAK), Bcl-2-like protein 11 (Bim) and p53-upregulated modulator of apoptosis (PUMA), serve critical roles in the P53-mediated apoptotic pathway, which can be inhibited by inhibitor of apoptosis proteins (IAPs), such as survivin (8). By contrast, the anti-apoptotic Bcl-2 family proteins, such as Bcl-2, Bcl-extra large (Bcl-xL) and myeloid cell leukemia sequence-1 (Mcl-1), are associated with the outer mitochondrial membrane, antagonize pro-apoptotic proteins and protect cells from programmed cell death (PCD) (9). P53 can mediate transcriptional repression of anti-apoptotic genes, including the Bcl-2 gene and the IAP family member survivin (10,11). Eventually, the caspase family becomes involved in the apoptotic process, during which caspase-3 is activated by caspase-9, and then executes the apoptosis (12). Caspases exist in the cell as zymogens and are activated when the cell encounters external or internal stimuli. The IR-induced caspase cascade may also inactivate the poly(ADP-ribose) polymerase (PARP), an enzyme critical for repairing damaged DNA, in order to block DNA repair, thereby promoting IR-induced apoptotic cell death. Indeed, both PARP-1 and PARP-2 knockout mice exhibit severe deficiencies in DNA repair, showing increased sensitivity to alkylating agents or IR (13).

The Stat3, a member of the Stat family, is a transcription factor that transmits pro-survival signals from the surface of the cell to the nucleus, playing a key role in the development of human cancers (14). Cytokines, such as interleukin (IL)-6, may activate Stat3 through tyrosine phosphorylation to transactivate anti-apoptotic regulators, such as Bcl-2, Bcl-xL, and other apoptosis-related genes (15). The NF- κ B is a ubiquitous transcription factor that is associated with inflammatory and innate immune responses (16). NF- κ B is constitutively activated by various stimuli, including inflammatory cytokines, such as tumor necrosis factor (TNF)- α , IL-1 β , epidermal growth factor (EGF), insulin-like growth factor (IGF)-1, T and B-cell mitogens, bacteria and lipopolysaccharides, viruses, viral proteins, double-stranded RNA, and physical and chemical stress (17). Under normal physiological conditions, by binding to the inhibitory protein I κ B α in the cytoplasm, NF- κ B assumes an inactive form (18). Upon induction by various stimuli, I κ B α is ubiquitinated and degraded, thereby releasing NF- κ B to translocate from the cytoplasm to the nucleus. The activated NF- κ B in the nucleus regulates the transcription of a wide range of target genes associated with cell proliferation, survival and angiogenesis (19).

Although the Stat3 and NF- κ B signaling pathways described above contribute to the radioresistance of cancers, it is not clear how they are overridden by the P53-mediated pathways in radiosensitive cancer cells. In the present study, spontaneous radiosensitive and radioresistant PC cell lines were screened and their potential signaling pathways mediating radiosensitivity were investigated following irradiation. The current study aimed to provide a novel insight into the mechanisms underlying the radiosensitivity of PC cells, particularly the unique functions of adaptively expressed EGF and cyclin D1.

Materials and methods

Cell culture and reagents. The human PC cells SW1990, Capan-2, PANC-1, AsPC-1, BxPC-3 and CFPAC-1 were obtained from the Type Culture Collection of the Chinese Academy of Sciences (Shanghai, China). The cells were grown in Dulbecco's modified Eagle's medium (DMEM) supplemented with 10% fetal bovine serum (FBS) and maintained in a humidified 5% CO₂ atmosphere at 37°C. DMEM and FBS were obtained from Gibco; Thermo Fisher Scientific, Inc. (Waltham, MA, USA). The Annexin V-fluorescein isothiocyanate (FITC) Apoptosis Detection kit was purchased from BD Biosciences (San Jose, CA, USA). Recombinant human EGF was purchased from PeproTech, Inc. (Rocky Hill, NJ, USA). TRIzol reagent was purchased from Invitrogen (Thermo Fisher Scientific, Inc.). Cell Counting Kit-8 (CCK-8) was purchased from Dojindo Molecular Technologies, Inc. (Kumamoto, Japan).

Clonogenic assay. PC cells at various concentrations were plated into 6-well plates (Corning Inc., Corning, NY, USA), according to the dose of irradiation, and cultured for 24 h. After irradiation by X-rays at 0, 2, 4, 6, 8 and 10 Gy, the cells were cultured for 2 weeks at 37°C. The cells were washed three times with PBS, fixed with ice-cold methanol for 15 min, stained with 1% crystal violet solution (Sigma-Aldrich; Merck KGaA, Darmstadt, Germany) for 15 min, and rinsed in distilled water to remove the excess dye. The plates were allowed to dry prior to scanning. Only colonies of ≥ 50 cells were counted. Triplicate experiments were performed independently. The surviving fractions were determined as ratios of the plating efficiencies (PE = counted colonies/seeded cells $\times 100$) of the irradiated cells to the non-irradiated cells. The cell survival curves were fitted with the linear-quadratic equation of $SF = \exp [-(\alpha D + \beta D^2)]$ by optimizing variable parameters α and β .

X-ray irradiation. Human PC cell lines were irradiated by a linear accelerator (Elekta Medical Systems, Stockholm, Sweden) with 8-MV X-rays at a dose rate of 500 cGy/min, the cells were further incubated for different time periods, and then harvested for the subsequent experiments.

Cell proliferation assay. Cells were seeded into 96-well culture plates at a density of 5,000 cells/well and allowed to adhere for 24 h. After X-ray irradiation, the cells were incubated for different times in a humidified chamber at 37°C. Each day for 3 consecutive days, viable cells were evaluated with the CCK-8 assay, according to the manufacturer's instructions. CCK-8 solution was added to the cells in 96-well plates incubated at 37°C for an additional 1 h, and the absorbance at 450 nm was determined using a microplate reader (ELX800; Bio-Tek Instruments, Inc., Winooski, VT, USA).

Flow cytometric detection of the cell cycle. PC cells were harvested by trypsin. After centrifugation, cells were washed twice with PBS and fixed with ethanol for 1 h at -20°C. After washing twice with PBS, the cells were stained with a solution containing 5 mg/ml propidium iodide (PI) and 1 mg/ml RNase A (Sigma Aldrich; Merck KGaA) at 4°C for 30 min. The cell-cycle distribution was examined by flow cytometry

(BD Biosciences) and the proportion of cells in the G0-G1, S and G2-M phases was determined. Cell cycle analysis was performed using FlowJo 7.6.1 software (FlowJo LLC, Ashland, OR, USA).

Flow cytometric detection of apoptosis. Cells were cultured in growth medium for 12 h at a density of 2×10^5 cells per well in 6-well plates, and irradiated at the indicated doses. Apoptotic cells were quantified using an Annexin V-FITC/PI Apoptosis Detection kit and FACSCalibur flow cytometry (BD Biosciences). The cells were harvested by centrifugation after irradiation and washed twice with PBS. The cells were then resuspended in 100 μ l of Annexin V binding buffer, incubated with 5 μ l of Annexin V-FITC for 15 min at room temperature, and counterstained with PI (final concentration 1 μ g/ml). After the incubation period, the cells were diluted with 190 μ l of Annexin V binding buffer. A total of 10,000 counts were acquired per sample, and examined by flow cytometry (BD Biosciences). Cells in the early stages of apoptosis were Annexin V-positive, whereas cells that were Annexin V-positive and PI-positive were in the late stages of apoptosis.

Nuclear protein extraction. Nuclear protein extracts were obtained using the nuclear and cytoplasmic extraction kit (Thermo Fisher Scientific, Inc.). Cells were harvested with trypsin and then centrifuged at 500 x g for 5 min at 4°C. Cells were resuspended with PBS and centrifuged at 500 x g for 5 min at 4°C. The supernatant was discarded, followed by addition of ice-cold CER I solution. The tube was vortexed vigorously for 15 sec and incubated on ice for 10 min. Then, CER II solution was added, followed by vortexing for 5 sec and incubation for 1 min. After centrifugation at 16,000 x g for 5 min at 4°C, the supernatant (cytoplasmic extract) was collected and the insoluble fraction was washed with PBS. Finally, NER solution was added to the tube and vortexed for 15 sec four times, followed by centrifugation at 16,000 x g for 10 min at 4°C and collection of the supernatant (nuclear extract).

Western blotting. The treated cells were collected and washed twice with cold PBS. The cells were lysed in 200 μ l RIPA buffer (cat. no. 89900; Thermo Fisher Scientific, Inc.) and the lysates were incubated on ice for 30 min, vortexed and centrifuged at 14,000 x g for 15 min at 4°C. The supernatant was collected and protein concentration was determined using the Bradford assay. After addition of sample loading buffer, protein samples (20 μ g) were electrophoresed on a 10% SDS-polyacrylamide gel and then transferred to PVDF membranes (Millipore Corporation, Billerica, MA, USA). After blocking for 4 h in a solution of 5% non-fat dry milk in Tris-buffered saline containing 0.1% Tween-20 (TBST) at room temperature for 1.5 h, the membranes were incubated overnight at 4°C with primary antibodies (1:1,000 dilution). The antibodies were: p53 (cat. no. sc-126; Santa Cruz Biotechnology, Inc., Dallas, TX, USA), PUMA (cat. no. 4976), BAX (cat. no. 5023), BAK (cat. no. 6947), Bcl-xL (cat. no. 2764), Bcl-2 (cat. no. 2870), PARP (cat. no. 9532), phosphorylated (p-) Histone H2AX (cat. no. 9718S), Survivin (cat. no. 2808), cyclin D1 (cat. no. 2978), p-EGF receptor (EGFR; cat. no. 3777), NF- κ B p65 (cat. no. 8242), p-NF- κ B p65 (cat. no. 3033), cleaved caspase-3

(cat. no. 9664), Stat3 (4 cat. no. 904), p-Stat3 (cat. no. 9145), β -actin (cat. no. 4970) (all from Cell Signaling Technology, Inc., Danvers, MA, USA), EGFR (cat. no. 18986-1-AP), TATA-binding protein (TBP; cat. no. 66166-1-Ig), and GAPDH (cat. no. 60004-1-Ig) (all from ProteinTech Group, Inc., Chicago, IL, USA). After washing four times, the membranes were incubated with secondary anti-rabbit and anti-mouse antibodies (cat. nos. 7074 and 7076; Cell Signaling Technology, Inc.; 1:3,000 dilution) at room temperature for 1 h. The blots were developed using an Immobilon Western Chemiluminescent detection reagent (Millipore Corporation) and the results were recorded using the ChemiDox XRS+ system (Bio-Rad Laboratories, Inc., Hercules, CA, USA). Quantitative analysis was performed using Image Lab 6.0.1 software (National Institutes of Health, Bethesda, MD, USA).

RNA interference. Small interfering (si)RNA targeting BAX, cyclin D1 and control siRNA were purchased from GenePharma Co., Ltd. (Shanghai, China). A total of 2×10^5 cells per well were seeded in 6-well plates and incubated overnight, followed by transfection with BAX siRNA-1 (5'-ACUUUGCCAGCAAACU GGUGCUGAA-3' and 5'-UUGAGCACCAGUUUGCUGGCAAAGU-3'), BAX siRNA-2 (5'-ATCCAGGATCGAGCAGGCG-3' and 5'-GGTTCTGATCAGTTCCGGCA-3'), cyclin D1 siRNA-1 (5'-CCCGCACGAUUUCAUUGAATT-3' and 5'-UUCAAUGAAAU CGUGCGGGTT-3'), cyclin D1 siRNA-2 (5'-GUCUGCGAGGAACAGAAGUTT-3' and 5'-ACUUCUGUCCUCGCAGACTT-3'), cyclin D1 siRNA-3 (5'-CCACAG AUGUGAAGUUCAUTT-3' and 5'-AUGAACUUCACAUCUGUGTT-3'), or negative control (5'-UUCUCCGAACGUGUCACGUTT-3' and 5'-ACGUGACACGUUCGGAGAATT-3'), using jetPRIME transfection reagent (Polyplus-transfection SA, Illkirch, France) according to the manufacturer's protocol. First, 110 pmole siRNA was diluted in 200 μ l of jetPRIME buffer and mixed by pipetting. Second, 4 μ l jetPRIME reagent was added, vortexed for 10 sec and spun down briefly, followed by incubation for 10 min at room temperature. Third, the transfection mixture was added dropwise to the cells in serum-containing medium, the plate was gently rocked, and then returned to the incubator. After 24 h, the transfection mixture was removed and fresh medium was added, and the cells were further cultured for 24 h.

RNA extraction and reverse transcription-quantitative polymerase chain reaction (RT-qPCR). Cells were seeded in 6-well plates and allowed to grow until semi-confluent prior to being irradiated in DMEM supplemented with 10% FBS. After treatment, total RNA was extracted using TRIzol reagent (Thermo Fisher Scientific, Inc.) according to the manufacturers' recommendations. cDNA was generated using equal amounts of sample RNA with RevertAid First strand cDNA Synthesis kit (Thermo Fisher Scientific, Inc.). Subsequently, 2 μ l of cDNA and Taq PCR Master Mix (Takara Biotechnology Co., Ltd., Dalian, China) was used for PCR. The primers sequences used for qPCR were as follows: BAX, forward, AAGCTGAGCGAG TGTCTCAAG and reverse, CAAAGTAGAAAAGGGCGAC AAC; cyclin D1, forward, GTGTATCGAGAGGCCAAAGG and reverse, GCAACCAGAAATGCACAGAC; IGF-1, forward, TTCAACAAGCCCACAGGGTA and reverse, GCAATACAT CTCCAGCCTCCT; EGF, forward, GCTTCAGGACCACA ACCATT and reverse, GGCATAAACCATTCCCATCTG;

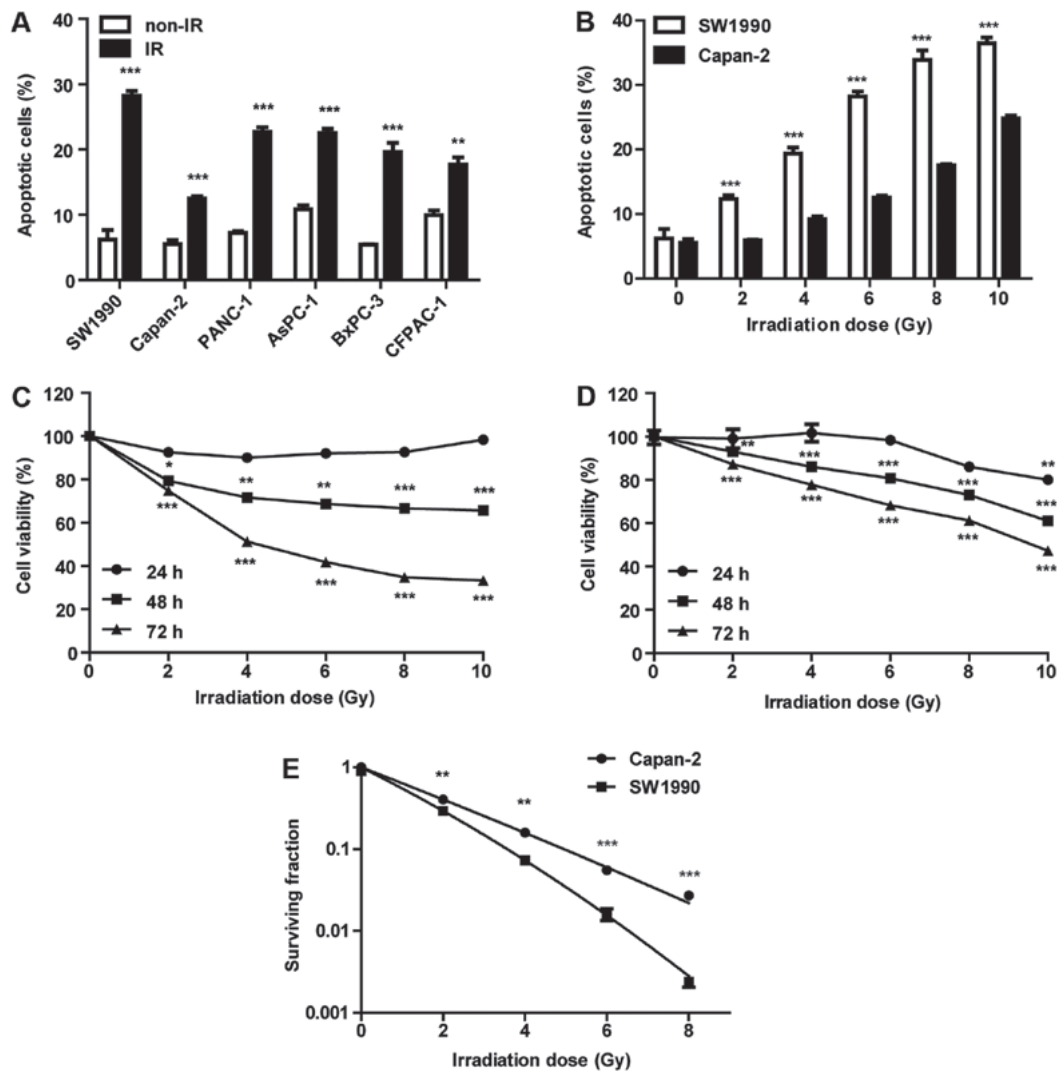


Figure 1. Identification of radiosensitive and radioresistant pancreatic cancer cells. (A) Different pancreatic cancer cells (SW1990, Capan-2, PANC-1, AsPC-1, BxPC-3 and CFPAC-1) were treated with 6 Gy and apoptosis was measured by flow cytometry. ** $P < 0.01$ and *** $P < 0.001$ vs. non-IR. (B) Both SW1990 and Capan-2 cells were treated with IR for 72 h and apoptosis was measured by flow cytometry. The data represent the mean \pm SEM of three independent experiments. *** $P < 0.001$ vs. irradiated Capan-2 cells. (C) SW1990 cells were analyzed for viability by the CCK-8 assay. * $P < 0.05$, ** $P < 0.01$ and *** $P < 0.001$ vs. non-IR. (D) Capan-2 cells were analyzed for viability by the CCK-8 assay. ** $P < 0.01$ and *** $P < 0.001$ vs. non-IR. (E) Clone forming efficiency was evaluated using crystal violet staining on day 7 post-irradiation. The data represent the mean \pm SEM of three independent experiments. ** $P < 0.01$ and *** $P < 0.001$ vs. irradiated SW1990 cells. IR, ionizing radiation; CCK, cell counting kit; SEM, standard error of the mean.

IL-6, forward, CAATGAGGAGACTTGCCTGG and reverse, GGCATTTGTGGTTGGGTCAG; IGF-1R, forward, CCTGAAAGGAAGCGGAGAG and reverse, GGGTCGGTGATGTTG TAGGT; EGFR, forward, ATGCAGAAGGAGGCAAAGTG and reverse, AGGTCATCAACTCCCAAACG; IL-6R, forward, GGTGAGAAGCAGAGGAAGGA and reverse, TGGGAGGTGGAGAAGAGAGA; and GAPDH, forward ATGACATCAAGAAGGTGGTG and reverse, CATACCAGGAAATGAGCTTG. PCR amplifications were performed as follows: 5 min at 94°C, followed by 25 cycles of 30 sec at 94°C, 30 sec at 55°C, 30 sec at 72°C, and a final extension step at 72°C for 5 min. qPCR was performed using the StepOnePlus Real-Time PCR System (ABI, Applied Biosystems; Thermo Fisher Scientific, Inc.). Relative fold changes in mRNA expression were calculated using the formula $2^{-\Delta\Delta C_q}$.

Statistical analysis. All statistical analyses were performed using GraphPad Prism 5.0 software (GraphPad Software, Inc.,

La Jolla, CA, USA). Each experiment was performed three times. All data are expressed as mean \pm standard error of the mean, unless otherwise specified. Comparison of data between two groups was performed using a two-tailed Student's *t*-test. Multiple comparisons were assessed by one-way analysis of variance with Bonferroni's post hoc test. $P < 0.05$ was considered to indicate a statistically significant difference.

Results

Identification of radiosensitive and radioresistant PC cells.

To evaluate the radiosensitivity of PC cells, six human PC cell lines (SW1990, Capan-2, PANC-1, AsPC-1, BxPC-3 and CFPAC-1) were irradiated with 6 Gy, and apoptotic cell rates were measured by flow cytometry 72 h post-IR. As illustrated in Fig. 1A, the SW1990 cell line was most sensitive to IR, whereas the Capan-2 cell line was the most resistant. The PANC-1, AsPC-1, BxPC-3 and CFPAC-1 cell lines exhibited

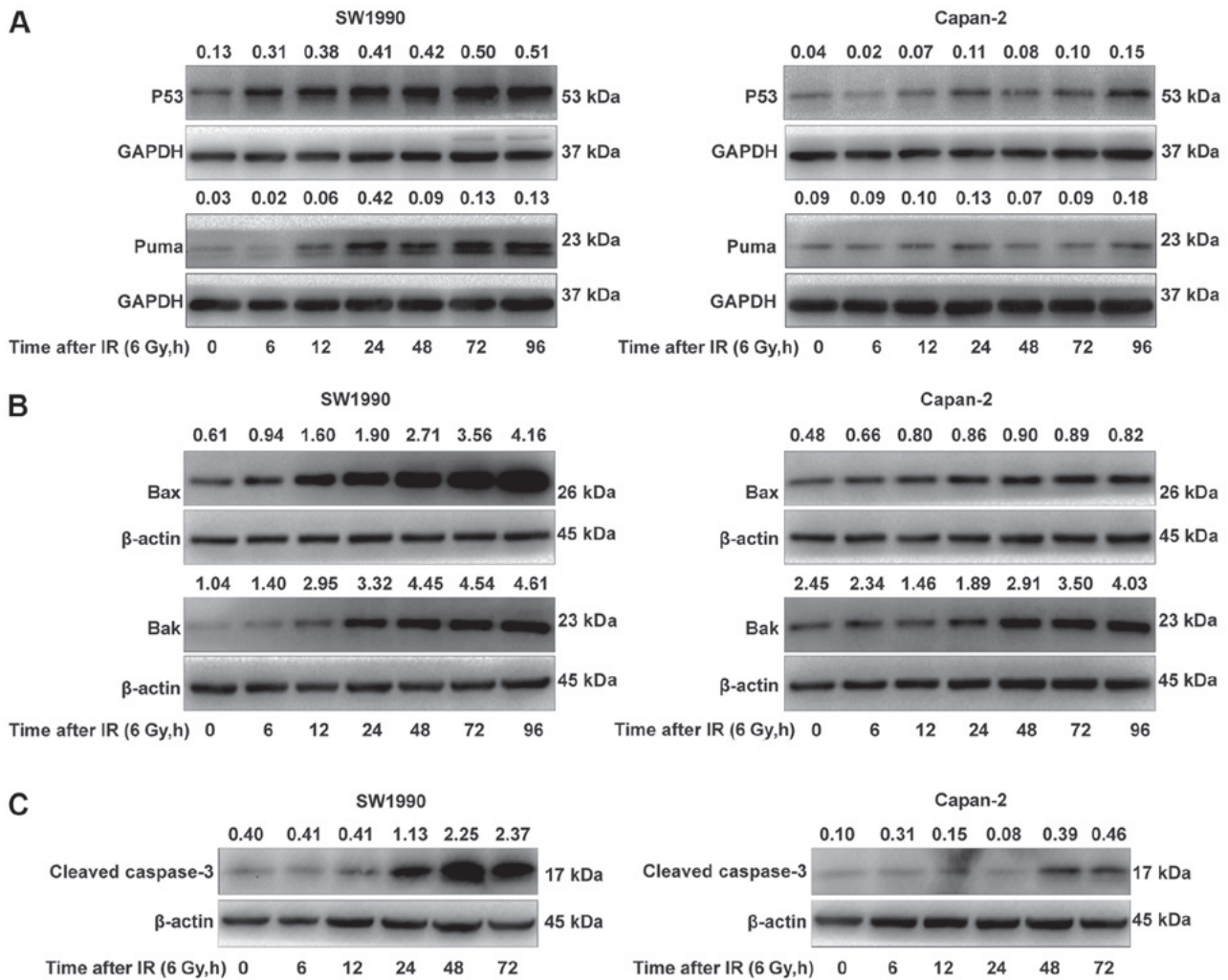


Figure 2. Activation of the P53-mediated apoptotic pathway is more pronounced in radiosensitive compared with radioresistant pancreatic cancer cells following ionizing radiation. Cells were irradiated and protein expression was analyzed by western blotting at the indicated time-points. (A) Representative blots for P53 and PUMA protein expression. GAPDH was used as a loading control. (B) BAX and BAK protein expression. β -actin was used as a loading control. (C) Cleaved caspase-3 protein expression. β -actin was used as a loading control. BAX, Bcl-2-associated X; BAK, Bcl-2 homologous antagonist/killer; PUMA, p53-upregulated modulator of apoptosis. Numbers above the bands indicate quantified protein levels normalized to loading control.

comparable but relatively mild sensitivity to IR. Thus, SW1990 and Capan-2 cells were irradiated with various doses (2, 4, 6, 8 and 10 Gy) and their viability was measured at 24, 48 and 72 h post-IR (Fig. 1C and D). Within 24 h post-IR, the viability of SW1990 and Capan-2 cells was not significantly affected. However, cell viability was significantly decreased in a dose-dependent manner at 24 h post-IR ($P < 0.001$). At 72 h post-IR, the viability of SW1990 cells was decreased more obviously compared with Capan-2 cells (Fig. 1C and D), confirming that SW1990 was the most sensitive cell line and Capan-2 was the most resistant cell line to IR. While SW1990 cells had a rate of spontaneous apoptosis comparable with Capan-2 cells in the culture prior to IR, their apoptosis rate increased ~ 2 -fold that of Capan-2 cells post-IR (Fig. 1B), suggesting a differential adaptive response of these cells to IR. Clonogenic formation assay was performed to examine its association with radiosensitivity. The survival fraction results revealed that SW1990 cells were more radiosensitive compared with Capan-2 cells post-IR ($P < 0.001$; Fig. 1E). Therefore, SW1990 cells were identified as radiosensitive and Capan-2 cells as radioresistant, and were used as a cell

model to investigate the molecular mechanisms underlying the adaptive radiosensitivity of PC cells in the present study.

Activation of the P53-mediated apoptotic pathway is more pronounced in radiosensitive compared with radioresistant PC cells post-IR. To elucidate the reason as to why SW1990 cells were more sensitive to IR compared with Capan-2 cells, the adaptive expression of the P53 protein in SW1990 cells and Capan-2 cells was examined following IR treatment. P53 is a major sensor of DNA damage mediating IR-induced cell death. While the basal levels of P53 protein were comparable between SW1990 and Capan-2 cells prior to IR, the P53 protein levels in the SW1990 cells were upregulated to a markedly higher extent compared with Capan-2 cells between 6 and 96 h post-IR (Fig. 2A). Consequently, PUMA, a protein downstream of P53 activation (20), was also upregulated in a similar manner in SW1990 cells post-IR (Fig. 2A). Additionally, the expression of BAX and BAK, two proapoptotic proteins that interact with PUMA to mediate the mitochondrial apoptosis pathway (21), was also upregulated, with kinetics similar to that of P53 and PUMA (Fig. 2B).

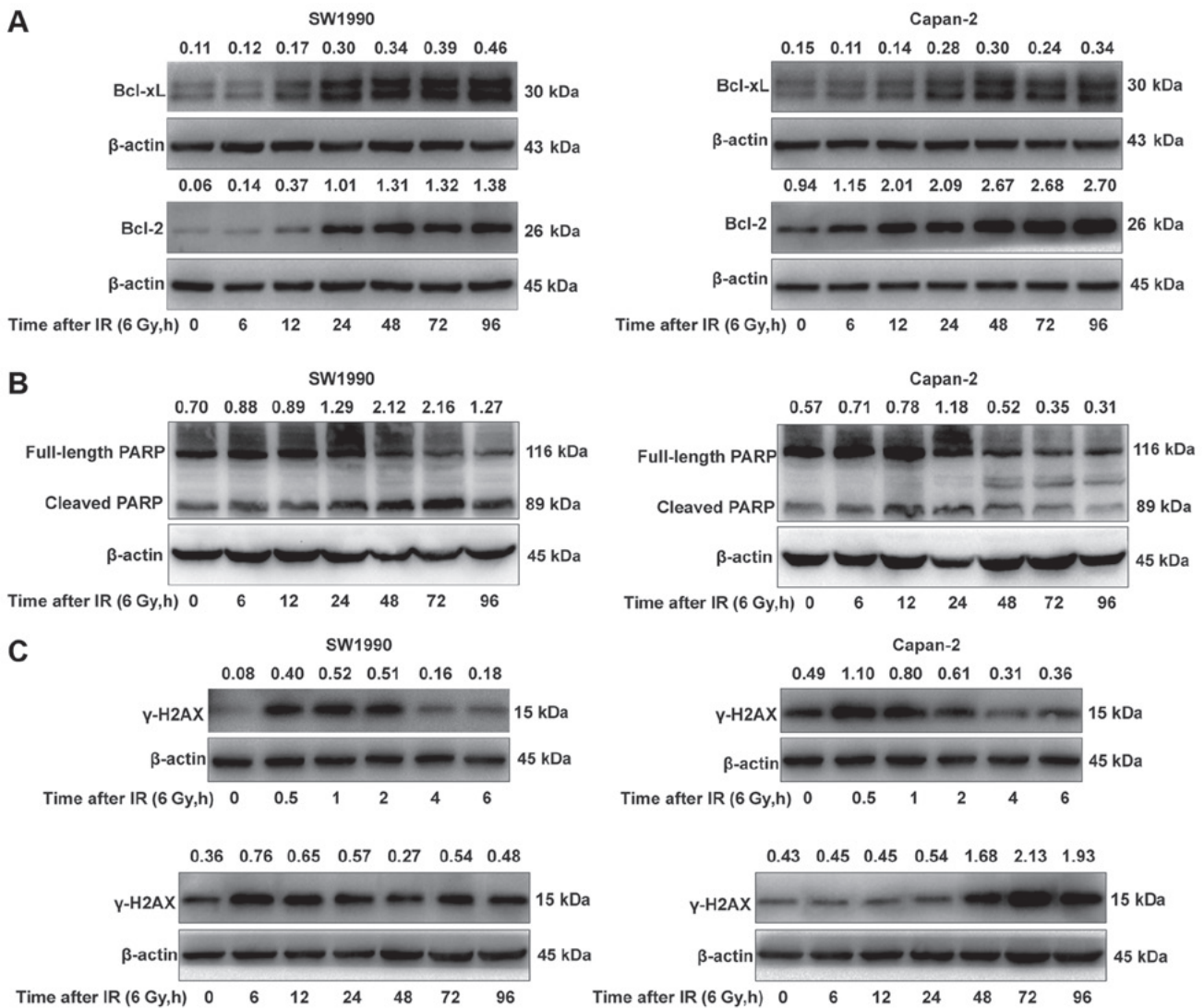


Figure 3. P53-mediated apoptotic pathway activation in radiosensitive pancreatic cancer cells is associated with inactivation of PARP. Cells were irradiated and protein expression was analyzed by western blotting at the indicated time-points. (A) Representative blots for Bcl-xL and Bcl-2 protein expression. (B) PARP protein expression. The protein bands at 116 kDa are specific for full-length PARP and the smeared signal above the full-length PARP is non-specific. Therefore, only the changes in the specific protein bands were measured. (C) γ-H2AX protein expression. β-actin was used as a loading control. PARP, poly(ADP-ribose) polymerase; Bcl-2, B-cell lymphoma-2; Bcl-xL, Bcl-extra large; γ-H2AX, γ-H2A histone family member X. Numbers above the bands indicate quantified protein levels normalized to loading control.

By contrast, P53, PUMA, BAX and BAK were less or not upregulated in Capan-2 cells post-IR (Fig. 2A and B). As a consequence, caspase-3, an executor of cell apoptosis, was also more markedly activated/cleaved in the radiosensitive SW1990 cells compared with the radioresistant Capan-2 cells, starting from 24 h post-IR (Fig. 2C). These results indicated that the P53-mediated mitochondrial apoptosis pathway was more extensively upregulated in the radiosensitive SW1990 cells compared with the radioresistant Capan-2 cells.

P53-mediated apoptotic pathway activation in radiosensitive PC cells is associated with inactivation of PARP. Enhanced activation of the P53/PUMA/BAX/BAK/caspase-3 pathway is considered to be associated with the suppressed expressions of Bcl-2 and Bcl-xL in the radiosensitive PC cells following IR treatment. To test this hypothesis, the adaptive expression of Bcl-2 and Bcl-xL was further examined in SW1990 and Capan-2 cells post-IR, as Bcl-2 and Bcl-xL can bind BAX or

BAK to suppress their functions. Unexpectedly, the expressions of Bcl-2 and Bcl-xL were not significantly decreased in the radiosensitive SW1990 cells compared with the radioresistant Capan-2 cells post-IR, although the basal level of Bcl-2 was higher in the radioresistant Capan-2 cells (Fig. 3A). The results indicated that the enhanced activation of the P53/PUMA/BAX/BAK pathway was likely not associated with the expression of Bcl-2 and Bcl-xL in radiosensitive PC cells, and other mechanisms may be responsible.

It is known that IR-induced DNA damage activates PARP to repair the damaged DNA, however activated caspase-3 may cleave PARP to block the DNA repair, and the failure to repair the damaged DNA may lead to cell death (22). Thus, the activation state of PARP was examined in SW1990 cells and Capan-2 cells post-IR. As illustrated in Fig. 3B, the cleaved PARP levels were higher in the radiosensitive SW1990 cells compared with the radioresistant Capan-2 cells at 72 h post-IR, suggesting that PARP was cleaved by activated caspase-3 in SW1990 cells but

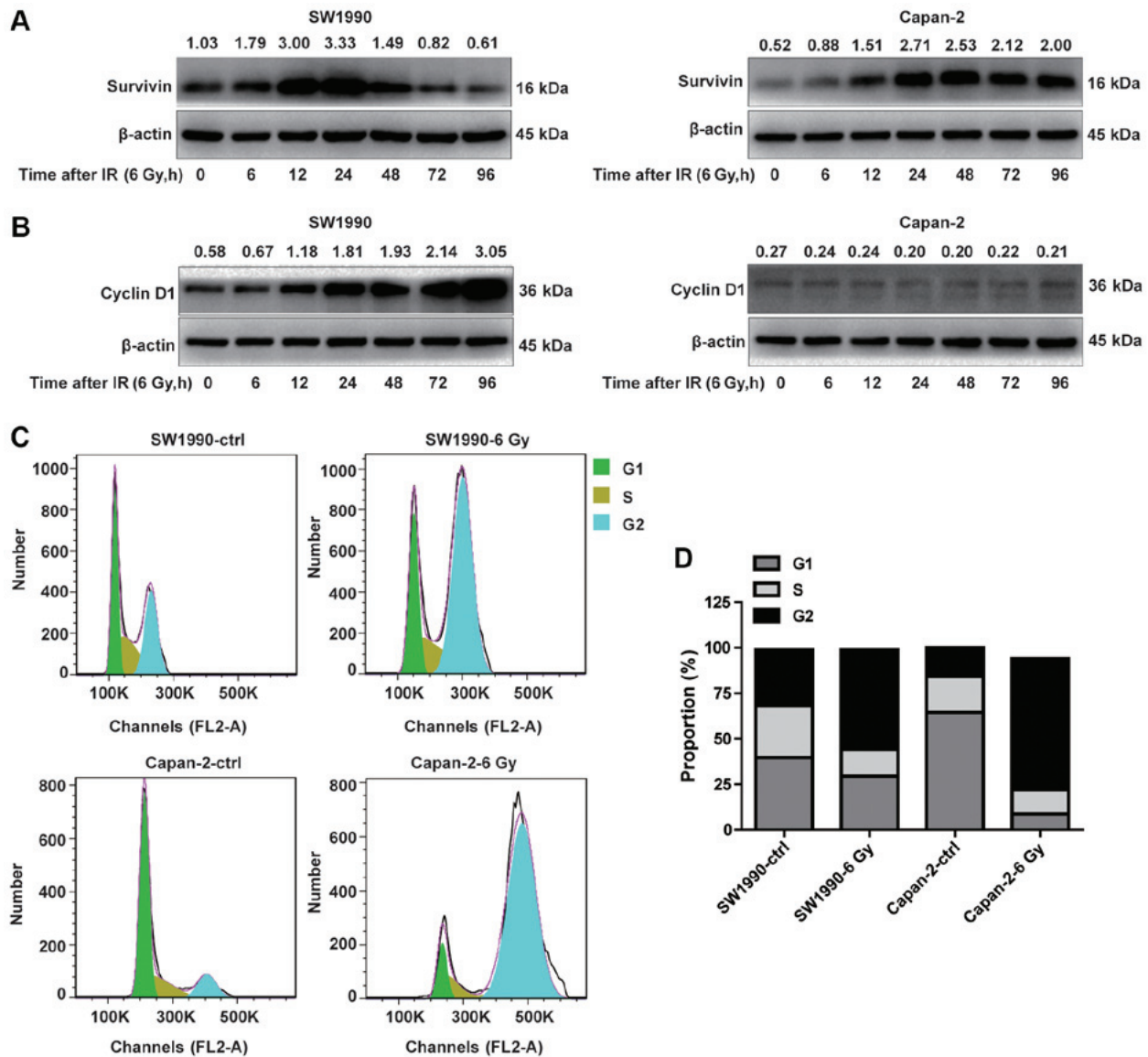


Figure 4. Cyclin D1 and survivin are distinctly expressed in radiosensitive and radioresistant pancreatic cancer cells. Cells were irradiated and protein expression was analyzed by western blotting at the indicated time-points. (A) Survivin and (B) cyclin D1 protein expression. β -actin was used as a loading control. (C) Cell cycle distribution was measured by flow cytometry with propidium iodide staining. Representative plots are shown. (D) Proportion of cells in G1, S and G2-M phases following irradiation. Numbers above the bands indicate quantified protein levels normalized to loading control.

not in Capan-2 cells. As a consequence, the DNA damage repair was blocked by the cleaved PARP in SW1990 cells, resulting in increased apoptosis or increased sensitivity to IR (Fig. 1). This hypothesis was further confirmed by the decreased expression of γ -H2A histone family member X (γ -H2AX), a marker of the efficiency of DNA repair (23), in SW1990 cells at 72 h post-IR, as compared to that in Capan-2 cells (Fig. 3C). At this time, SW1990 cells were more susceptible to radiation-induced cell death (Fig. 1B-D). Notably, there were two peaks of γ -H2AX expression in both radiosensitive and radioresistant PC cells within 96 h post-IR. The first peak appeared between 0.5 and 2 h post-IR, and the second peak between 6 and 12 h or between 48 and 96 h post-IR in the radiosensitive SW1990 cells (Fig. 3C). The expression kinetics of γ -H2AX was essentially consistent with that of cleaved PARP (Fig. 3B). These results indicated that the enhanced activation of the P53/PUMA/BAX/BAK/caspase-3 pathway following IR may sensitize PC cells through cleaving PARP to block DNA damage repair.

Cyclin D1 and survivin are distinctly expressed in radiosensitive and radioresistant PC cells. To determine whether the activation of the P53/PUMA/BAX/BAK/caspase-3 pathway in radiosensitive PC cells was associated with the downregulation of IAPs, the adaptive expression of survivin, a member of the IAP family, was investigated in radioresistant and radiosensitive cancer cells. As illustrated in Fig. 4A, survivin appeared to be distinctively expressed in SW1990 and Capan-2 cells post-IR. While survivin was constitutively expressed in Capan-2 cells at a higher level compared with SW1990 cells (Fig. 4A), it was transiently upregulated in SW1990 cells between 12 and 24 h post-IR, followed by a marked downregulation starting from 48 h, resulting in levels lower than Capan-2 cells. The downregulation of survivin was associated with the upregulation of P53, PUMA, BAX and BAK, and cleaved caspase-3 (Fig. 2) in SW1990 cells. By contrast, survivin was increasingly upregulated in Capan-2 cells post-IR, without a subsequent decrease after 48 h,

suggesting that the P53-mediated apoptotic pathway was inhibited by survivin in the radioresistant PC cells (Fig. 4A). These results suggest that adaptive expression of survivin is transient in radiosensitive cancer cells but persistent in radioresistant cells, serving a critical role in modulating the radiosensitivity of PC cells.

It is well-known that survivin is specifically expressed in dividing cancer cells at the G2/M cell cycle phase, during which time cyclin D1 is downregulated (24). Thus, we investigated whether the adaptive expression of survivin in radioresistant PC cells was associated with decreased expression of cyclin D1, a marker of G1/S phase (25), and vice versa. As illustrated in Fig. 4B, the expression pattern of cyclin D1 was opposite to that of survivin in the radiosensitive SW1990 cells within 96 h post-IR, whereas cyclin D1 expression was suppressed in radioresistant PC cells (Fig. 4B). The kinetics of the adaptive expression of cyclin D1 was similar to that of P53, PUMA, BAX and BAK in SW1990 cells (Fig. 2A and B). These results suggested that cyclin D1 and survivin were oppositely expressed in radiosensitive and radioresistant PC cells.

Since cyclin D1 and survivin are specifically expressed during the G1/S and G2/M phases, respectively, the cell cycle status of the SW1990 and Capan-2 cells was examined at 24 h post-IR. The % of G1/S phase cells (68.06%) was decreased in SW1990 cells compared with Capan-2 cells (84.15%) prior to IR. By contrast, the % of G2/M phase cells was markedly higher (30.94%) in SW1990 cells compared with Capan-2 cells (15.92%) prior to IR (Fig. 4C and D). This cell cycle pattern was reversed following IR treatment, with more SW1990 cells arrested at the G1/S phase, and more Capan-2 cells arrested at the G2/M phase (Fig. 4C and D). These results suggested that the survivin-associated G2/M phase cells were less susceptible to IR-induced cell death compared with the cyclin-D1-associated G1/S phase cells. Therefore, the adaptive expression levels of cyclin D1 and survivin in PC cells after IR may determine the susceptibility of cancer cells to radiation-induced cell death.

EGF and IL-6/IGF-1 are distinctly expressed in radiosensitive and radioresistant PC cells. Since the expression of cyclin D1 and survivin is regulated by growth factors such as EGF, IL-6 and IGF-1 (26-31), their expression was examined in the radiosensitive and radioresistant PC cells following exposure to IR. As illustrated in Fig. 5A, EGF transcripts were constitutively expressed and adaptively upregulated in the radiosensitive SW1990 cells, but less in the radioresistant Capan-2 cells post-IR. By contrast, IGF-1 and IL-6 were constitutively expressed and adaptively upregulated in the radioresistant Capan-2 cells, but less so or not at all in the radiosensitive SW1990 cells (Fig. 5D and F). Notably, EGFR transcripts were constitutively expressed at a higher level in Capan-2 cells compared with SW1990 cells (Fig. 5B). At the protein level, EGFR also appeared to be less expressed in SW1990 cells. However, the levels of p-EGFR were significantly upregulated in Capan-2 cells post-IR, while they were less or not upregulated in SW1990 cells (Fig. 5C). Therefore, the adaptively increased expression of EGF and activation of EGFR appeared to be associated with cell proliferation and survival. These results suggested that the adaptively upregulated EGF may be associated with the upregulation of cyclin D1 in radiosensitive PC cells post-IR (Fig. 4B).

Of note, similar to EGF expression, the adaptive upregulation of IGF-1 and IL-6 in the radioresistant Capan-2 cells was not necessarily correlated with the IGF-1R and IL-6R. The IL-6R mRNA was upregulated in SW1990 cells, while the IGF-1R mRNA levels were comparable between SW1990 and Capan-2 cells (Fig. 5E and G). The NF- κ B protein, a downstream signaling protein of IGF-1, was differentially activated in SW1990 and Capan-2 cells. The activated NF- κ B (p65) protein (p-p65) was detected in the cytoplasm (Fig. 5H) and nuclei (Fig. 5I) of Capan-2 cells more prominently compared with SW1990 cells. In addition, Stat3, which is induced and activated by IL-6, was more highly expressed in Capan-2 cells compared with SW1990 cells before and after IR (Fig. 5J). These results indicated that IGF-1 and IL-6, rather than EGF, may contribute to the radioresistance of PC cells through activation of the NF- κ B and Stat3 pathways, respectively.

Adaptive expression of EGF is required for sensitization of PC cells through activation of the cyclin D1/P53 pathway. Since cyclin D1 and EGF were adaptively upregulated in the radiosensitive SW1990 cells with similar kinetics, we investigated whether adaptive expression of EGF could induce cyclin D1 expression in radioresistant cancer cells. To test this hypothesis, exogenous EGF was added into the cultures of the radioresistant Capan-2 cells and its effects on cyclin D1 expression in the radioresistant cells were examined at 72 h post-IR. As illustrated in Fig. 6, exogenous EGF promoted cyclin D1 expression in Capan-2 cells at 72 h post-IR (Fig. 6B), suggesting that continuous supply (autocrine) of EGF may be required for the radioresistant PC cells to continuously express cyclin D1. As a control, addition of exogenous EGF to SW1990 cells exerted no additive effect on the expression of cyclin D1 at 72 h post-IR (Fig. 6B). Consistently with cyclin D1 expression, exogenous EGF also promoted P53 expression in Capan-2 cells at 72 h post-IR, although to a relatively lower extent compared with the SW1990 cells (Fig. 6A). The enhanced P53 expression was associated with decreased γ -H2AX expression (Fig. 6C). These results were supported by the fact that exogenous EGF promoted IR-induced cell death in Capan-2 cells, although moderately (Fig. 6D). Therefore, the adaptive expression of EGF may sensitize cancer cells to IR through upregulation of cyclin D1 and P53.

Knockdown of cyclin D1 and BAX prevents IR-induced apoptotic cell death. To further confirm that the EGF-dependent expression of cyclin D1 is critically involved in the radiosensitization of cancer cells, cyclin D1 or BAX were silenced by siRNA in SW1990 and Capan-2 cells, in order to examine their effects on apoptotic cell death of PC cells upon IR exposure. First, it was confirmed that cyclin D1 and BAX were transcriptionally upregulated in SW1990 cells but less so in Capan-2 cells upon IR exposure (Fig. 7A and B). These data were in accordance with the results observed for the protein levels in Fig. 4. siRNAs specific for cyclin D1 and BAX were screened and used for subsequent experiments (Fig. 7C and D). Cyclin D1 knockdown resulted in decreased P53 in SW1990 cells after irradiation (Fig. 7E). However, the expression of P53 was not significantly downregulated in Capan-2 cells (Fig. 7E). Consistently, the % of apoptotic cells was decreased in the radiosensitive SW1990 cells, but not in the radioresistant Capan-2 cells post-IR (Fig. 7F). However, BAX knockdown

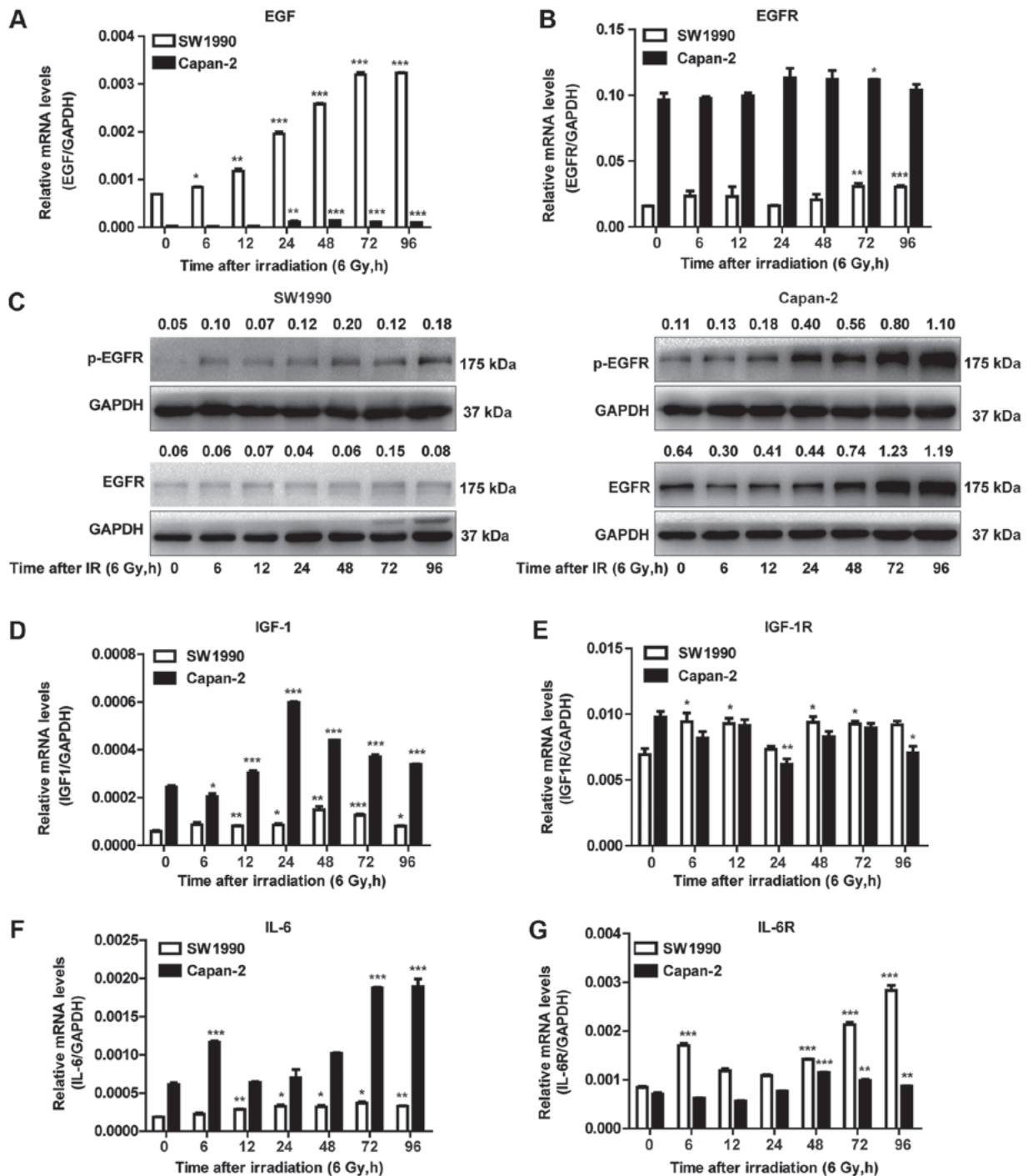


Figure 5. EGF and IL-6/IGF-1 are distinctly expressed in radiosensitive and radioresistant pancreatic cancer cells. (A) RT-qPCR was performed to measure the mRNA expression of EGF. * $P < 0.05$, ** $P < 0.01$ and *** $P < 0.001$ vs. non-IR. (B) RT-qPCR was performed to measure the mRNA expression of EGFR. * $P < 0.05$, ** $P < 0.01$ and *** $P < 0.001$ vs. non-IR. (C) Western blot analysis was performed using antibodies against the p-EGFR and total EGFR. GAPDH was used as a loading control. (D) RT-qPCR of IGF-1 levels. * $P < 0.05$, ** $P < 0.01$ and *** $P < 0.001$ vs. non-IR. (E) RT-qPCR of IGF-1R levels. * $P < 0.05$ and ** $P < 0.01$ vs. non-IR. (F) RT-qPCR of IL-6 levels and (G) RT-qPCR of IL-6R levels. ** $P < 0.01$ and *** $P < 0.001$ vs. non-IR.

resulted in decreased apoptosis in both SW1990 and Capan-2 cells (Fig. 7G). These results confirm that cyclin D1 has an important role in the radiosensitization of PC cells.

Discussion

Radiotherapy is one of the common approaches to the treatment of cancer, including PC. IR induces cancer cell apoptosis, however, irradiation can also induce various responses, such

as radioresistance, which may contribute to tumor recurrence and metastasis (32). It has been reported that cancer cells can adaptively respond to irradiation by regulating several signaling pathways, including those mediated by P53, Stat3 and NF- κ B (33-35). It is well-known that the P53-mediated pathway is enhanced, but the Stat3 and NF- κ B-mediated pathways are suppressed, in radiosensitive cancer cells. However, it remains unclear how these pathways are differentially regulated and utilized in radiosensitive vs. radioresistant cancer cells. To the

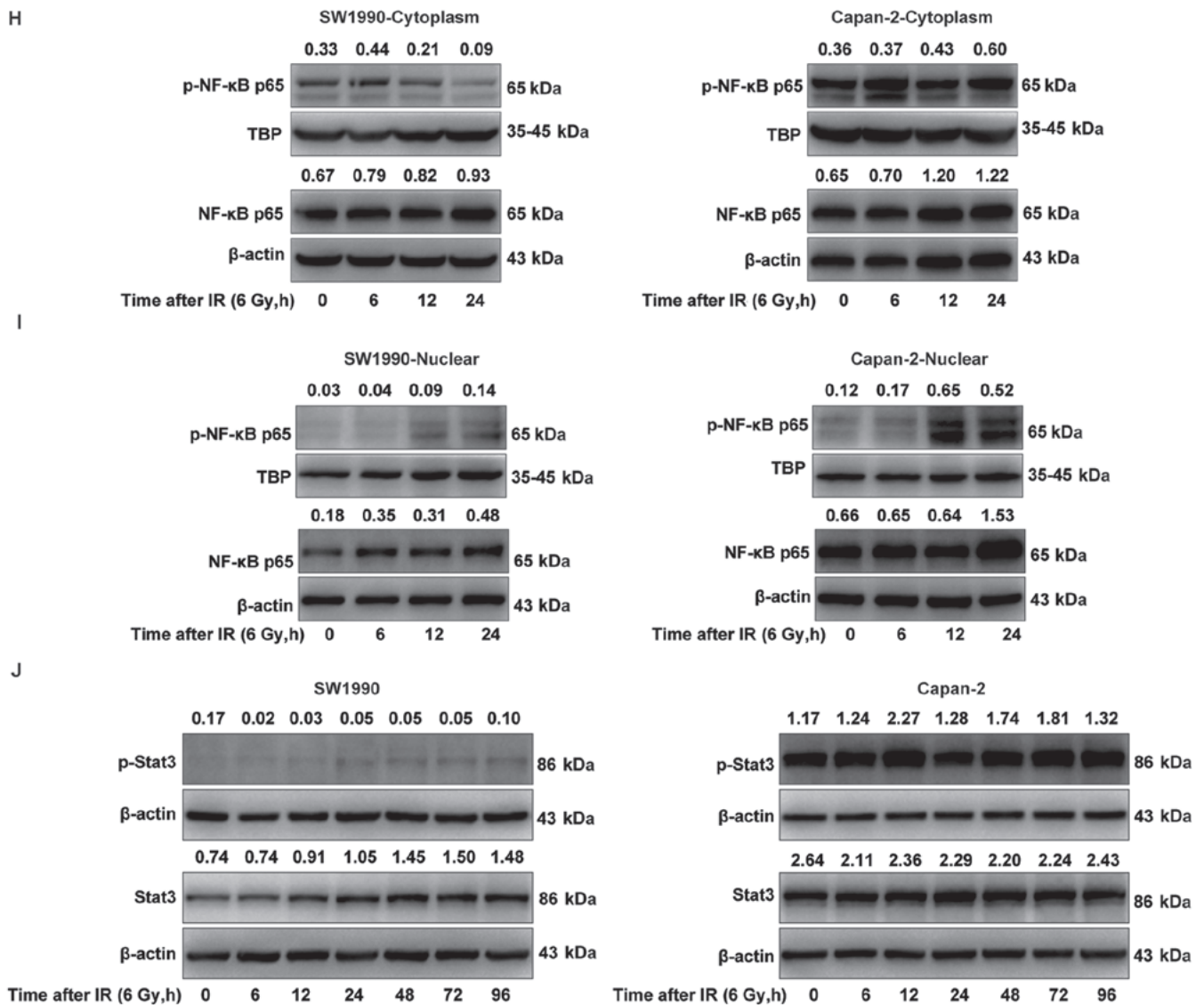


Figure 5. Continued. (H) Western blot analysis was performed using antibodies against NF-κB p65 and NF-κB p-p65. β-actin was used as a loading control for cytoplasmic protein. (I) Western blot analysis was performed using antibodies against the NF-κB p65 and NF-κB p-p65. TBP was used as a loading control for nuclear protein. (J) Western blot analysis was performed using antibodies against p-Stat3 and total Stat3. β-actin was used as a loading control. EGF, epidermal growth factor; IL, interleukin; IGF, insulin-like growth factor; RT-qPCR, reverse transcription-quantitative polymerase chain reaction; EGFR, EGF receptor; p-, phosphorylated; IGF-1R, IGF-1 receptor; IL-6R, IL-6 receptor; NF, nuclear factor; TBP, TATA-binding protein; Stat, signal transducer and activator of transcription. Numbers above the bands indicate quantified protein levels normalized to loading control.

best of our knowledge, the present study is the first to demonstrate that the radiosensitivity of PC cells may be determined and modulated at least partially by the status of adaptive expression of EGF or IL-6 and IGF-1 in irradiated cancer cells (Fig. 8). In radiosensitive cancer cells, the adaptively expressed endogenous EGF may promote cyclin D1 expression, which in turn enhances the activity of the P53/PUMA/BAX/caspase-3 pathway, reducing survivin expression and eventually preventing DNA repair through inactivation of PARP. By contrast, the radioresistance of cancer cells may be mediated by the IGF-1 and/or IL-6 pathways, which is characteristic of increased activation of Stat3 and NF-κB, respectively. Furthermore, the P53-mediated apoptotic pathway is suppressed by survivin in radioresistant cancer cells (Fig. 8). These findings are of great significance in understanding the mechanisms underlying the radiosensitivity of cancer cells and providing valuable prognostic and therapeutic markers for cancer radiotherapy.

A number of proapoptotic and antiapoptotic factors have been reported to be involved in the radiosensitivity of cancer cells. P53 can initiate apoptosis and programmed cell death, if DNA damage proves to be irreparable. The present study provided evidence that P53-mediated apoptosis of cancer cells post-IR is associated with inactivation of PARP, and thus irreparable DNA damage. P53 and its downstream signaling proteins PUMA, BAX, BAK and caspase-3 were more active in the radiosensitive SW1990 cells compared with the radioresistant Capan-2 cells. In particular, the kinetics of caspase-3 activation was similar to that of PARP inactivation, suggesting that caspase-3 inactivated PARP, leading to failure of DNA repair and cell death. The DNA damage-dependent PARP activation is an immediate cellular response to metabolic, chemical, or radiation-induced DNA damage. Both PARP-1 and PARP-2 knockout mice exhibit severe deficiencies in DNA repair mechanisms, with ensuing increased sensitivity

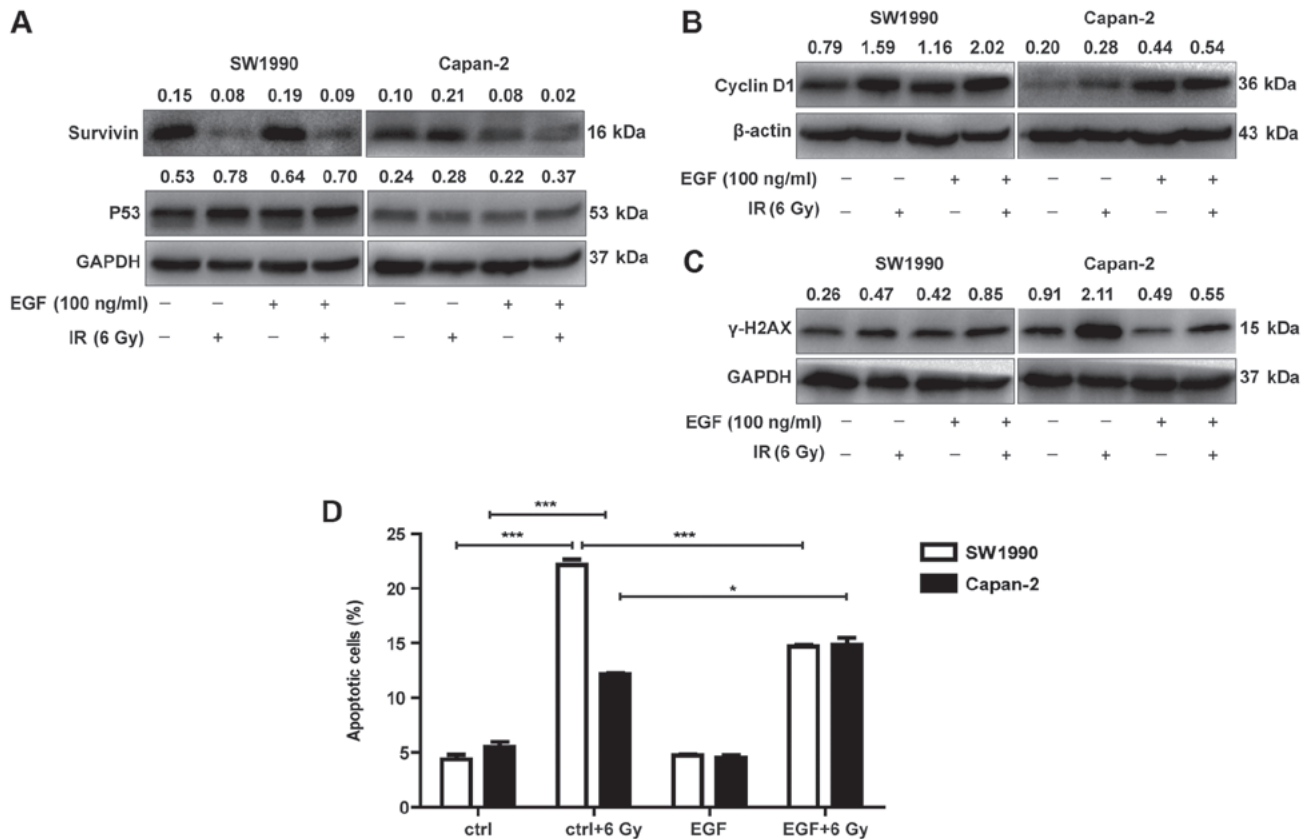


Figure 6. Adaptive expression of EGF is required for the sensitization of pancreatic cancer cells through activation of the cyclin D1/P53 pathway. (A) Western blot analysis was performed using antibodies against survivin and P53. GAPDH was used as a loading control. (B) Western blot analysis was performed using antibodies against cyclin D1. β-actin was used as a loading control. (C) Western blot analysis was performed using antibodies against γ-H2AX. GAPDH was used as a loading control. (D) Apoptosis was measured by flow cytometry. The data represent the mean ± standard error of the mean of three independent experiments. *P<0.05 and ***P<0.001, with comparisons indicated by brackets. EGF, epidermal growth factor; γ-H2AX, γ-H2A histone family member X. Numbers above the bands indicate quantified protein levels normalized to loading control.

to alkylating agents or IR (36). PARP inactivation by cleaved caspase-3 may result in defective DNA repair in radiosensitive PC cells. However, the expressions of Bcl-2 and Bcl-xL was not defective in radiosensitive PC cells, suggesting that the Bcl-2-mediated antiapoptotic functions in these cells were unaffected. Therefore, the P53/PARP pathway may override the Bcl-2/Bcl-xL pathway in radiosensitive cancer cells upon exposure to IR.

There remains the question of how the P53/PARP pathway was modulated in radiosensitive vs radioresistant PC cells. Analysis of autocrine factors revealed that EGF and IGF-1/IL-6 were differentially expressed in radiosensitive and radioresistant PC cells after IR. This finding suggests that adaptive expression of EGF may single out the P53/PARP pathway and thus increase the radiosensitivity of cancer cells. Indeed, the kinetics of transcriptional expression of EGF is similar to that of P53 expression. In addition, the kinetics of cyclin D1 expression is also similar to P53, suggesting a functional association between EGF, P53 and cyclin D1. This hypothesis was confirmed by the fact that radioresistant Capan-2 cells became more apoptotic post-IR when exogenous EGF was added to the culture, which was accompanied by increased expression of cyclin D1 and P53. Of note, exogenous EGF exerted no further effects on the expression of P53 and cyclin D1 in the radiosensitive SW1990 cells post-IR, suggesting that endogenous EGF was sufficient to initiate the cyclin D1/P53/PARP pathway. Furthermore,

knockdown of cyclin D1 decreased P53 expression in the radiosensitive PC cells only following IR treatment. These results indicate that in radiosensitive cancer cells, EGF may be upregulated and in turn stimulate cyclin D1 expression followed by upregulation of P53 (EGF/cyclin D1/P53 pathway). Therefore, a mechanism was identified (namely the EGF/cyclin D1/P53/PUMA/BAX/caspase-3/PARP pathway), through which radiosensitive cancer cells may undergo apoptosis post-IR. However, this pathway is less or not activated in radioresistant cancer cells post-IR.

EGFR is usually overexpressed in various types of tumor cells, and mediates tumor cell proliferation, invasion, metastasis and resistance to radiotherapy and chemotherapy (37,38). It has been reported that EGFR can perform its function by translocating from the plasma membrane to the nucleus through two pathways (39-41). In addition to directing phosphorylation of proliferating cell nuclear antigen (PCNA) (42), nuclear EGFR can also interact with Stat3 and E2F1, regulating transcription of cyclin D1, inducible nitric oxide synthase (iNOS), MYB proto-oncogene like 2 (B-Myb) and Aurora kinase A (43-45). The present study revealed a distinct but opposite expression pattern of EGF/EGFR between radiosensitive and radioresistant PC cells. Adaptive expression of EGF transcripts was observed in radiosensitive but not in radioresistant PC cells. Furthermore, EGFR was expressed at a higher level in radioresistant

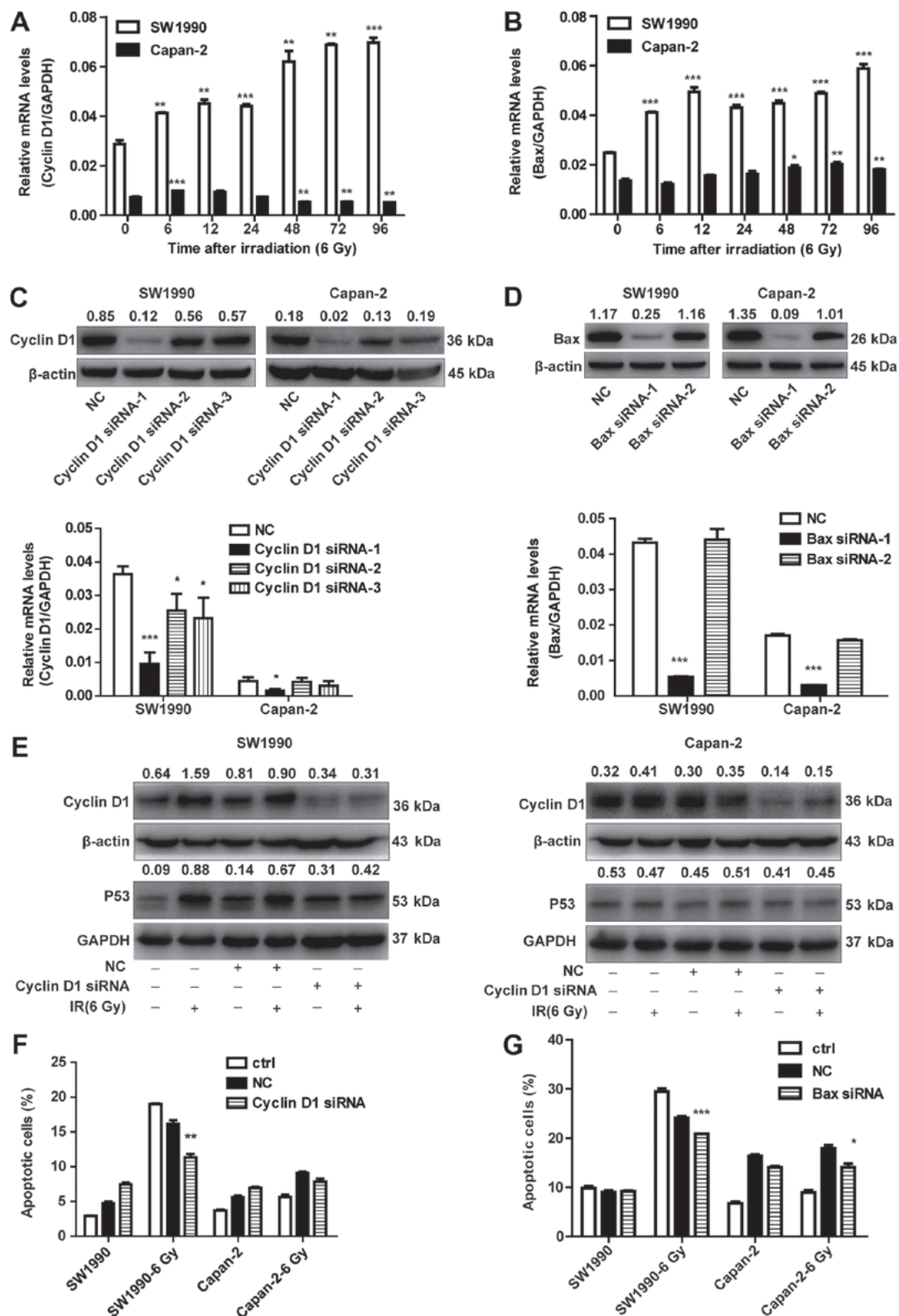


Figure 7. Knockdown of cyclin D1 and BAX prevents IR-induced apoptotic cell death. (A) RT-qPCR was performed to measure the cyclin D1 mRNA expression. $^{**}P<0.01$ and $^{***}P<0.001$ vs. non-IR. (B) RT-qPCR was performed to measure the BAX mRNA expression. $^{*}P<0.05$, $^{**}P<0.01$ and $^{***}P<0.001$ vs. non-IR. (C) The protein expression and mRNA levels of cyclin D1 and (D) Bax were measured by western blotting and RT-qPCR analysis, respectively, following siRNA transfection. $^{*}P<0.05$ and $^{***}P<0.001$ vs. NC. (E) Western blot analysis was performed using antibodies against cyclin D1 and P53. β -actin and GAPDH were used as loading controls. (F) Cell apoptosis was measured by flow cytometry. $^{**}P<0.01$ vs. irradiated NC cells. (G) Cell apoptosis was measured by flow cytometry. $^{*}P<0.05$ and $^{***}P<0.001$ vs. irradiated NC cells. BAX, Bcl-2-associated X; IR, ionizing radiation; RT-qPCR, reverse transcription-quantitative polymerase chain reaction; NC, negative control. Numbers above the bands indicate quantified protein levels normalized to loading control.

compared with radiosensitive cells. However, it is likely that a high level of endogenous EGF may promote p-EGFR

translocation to the nucleus to induce cyclin D1 transcription in radiosensitive PC cells, although the level of p-EGFR is low.

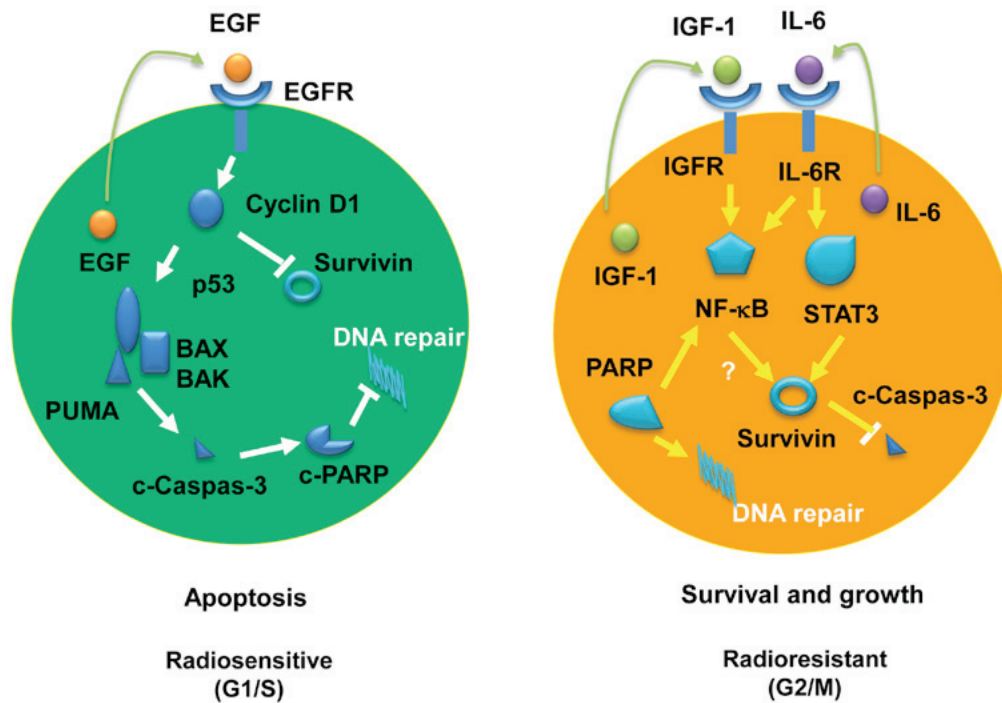


Figure 8. Schematic diagrams of the adaptive molecular pathways for radiosensitive and radioresistant pancreatic cancer cells. Left panel, radiosensitive pathway; right panel, radioresistant pathway. EGF, epidermal growth factor; BAX, Bcl-2-associated X; BAK, Bcl-2 homologous antagonist/killer; PUMA, p53-upregulated modulator of apoptosis; PARP, poly(ADP-ribose) polymerase; IGF, insulin-like growth factor; IL, interleukin; NF, nuclear factor; STAT, signal transducer and activator of transcription.

Consistent with this hypothesis, the present study observed that cyclin D1 was upregulated in the radiosensitive SW1990 cells compared with the radioresistant Capan-2 cells. However, the low levels of endogenous EGF may not be sufficient to stimulate EGFR translocation, despite the fact that EGFR is highly expressed in radioresistant Capan-2 cells. These results suggest that the level of autocrine expression of EGF is crucial for the cancer cells to acquire radiosensitivity upon irradiation.

Cyclin D1 is known to be involved in cell-cycle arrest in DNA-damage responses and it serves a key role in maintaining the integrity of the G1/S checkpoint via the activation of apoptotic pathways following exposure to IR *in vitro* (46). Cyclin D1 prevents cell apoptosis when it is sequestered in the cytoplasm, but may induce apoptosis when it is localized in the nucleus (47). The localization of cyclin D1 is associated with the radiation dose. It has been reported that high-dose of irradiation (5 Gy of γ -rays) may enhance cyclin D1 translocation from the cytoplasm to the nucleus. By contrast, low-dose of irradiation (10 cGy X-rays) may induce cyclin D1 accumulation in the cytoplasm by dissociating the complex of cyclin D1 and chaperone 14-3-3, as demonstrated in human keratinocytes (48). Furthermore, cyclin D1 can directly interact with the pro-apoptotic BAX protein to prevent apoptosis via improving the mitochondrial membrane potential ($\Delta\psi$) after irradiation. Blocking cyclin D1/BAX complexes using cyclin D1-specific siRNA reversed the mitochondrial membrane potential and suppressed the apoptotic response after irradiation. In the present study, it was demonstrated that knockdown of cyclin D1 using specific siRNAs promoted apoptosis in both radiosensitive and radioresistant PC cells, but decreased apoptosis in PC cells post-IR, especially more so in radiosensitive PC cells. These results suggest that radiation-induced cyclin D1 is more likely translocated to the nucleus, mediating cell death. However,

it is unlikely that cyclin D1 forms a complex with BAX to prevent apoptosis in radiosensitive cancer cells post-IR, although the levels of BAX were found to be high in the radiosensitive SW1990 cells. Further investigation is required to verify this hypothesis.

The present study demonstrated that cyclin D1 expression is mutually exclusive to survivin expression in a time-dependent manner, consistent with the kinetics of cell apoptosis post-IR. Cyclin D1 is expressed in the G1/S phase, whereas survivin is expressed in the G2/M phase (49). Increased cyclin D1 expression in the radiosensitive SW1990 cells was found to be associated with decreased expression of survivin at 48-72 h post-IR when cell apoptosis reaches a peak, suggesting that the cells arrested in the G1/S phase are more susceptible to apoptosis. By contrast, higher levels of survivin expression were observed in the radioresistant Capan-2 cells, suggesting that the radioresistant cells that have progressed to the G2/M phase are resistant to apoptotic cell death induced by irradiation. Therefore, cyclin D1 and survivin appear to be potential markers for evaluating the radiosensitivity of cancer cells.

While EGF is adaptively expressed in radiosensitive PC cells to mediate apoptosis post-IR, IL-6 and IGF-1 are adaptively expressed in radioresistant PC cells. Both IL-6 and IGF-1 are reportedly associated with radioresistance of cancer (50,51). IL-6, as an inflammatory cytokine, can activate the Janus kinase (Jak)/Stat3 signaling pathway in both a pro-inflammatory and an anti-inflammatory manner. In human esophageal carcinoma cells, IL-6 exerts its anti-apoptotic function through activation of both Stat3 and mitogen-activated protein kinase pathways (51). Constitutive activation of Stat3 leads to an increase in the oncogenes that drive proliferation and inhibit apoptosis (52). In addition, IL-6 can also activate the NF- κ B

pathway, further driving IL-6 production (53). IGF-1-mediated phosphoinositide 3-kinase (PI3K)/Akt signaling can enhance NF- κ B signaling (54), which exerts strong anti-apoptotic effects on cancer cells. In the present study, we also observed that Stat3 and NF- κ B were not only constitutively but also adaptively expressed and highly activated in radioresistant PC cells compared with radiosensitive PC cells, suggesting that both autocrine IL-6 and IGF-1 may coordinately have an important role in mediating radioresistance of PC cells upon IR exposure. The precise mechanisms through which IL-6 and IGF-1 interact to promote radioresistance of cancer cells require further investigation. In addition, these findings are based on cell models *in vitro*, and therefore further verification will be required in patients undergoing radiotherapy.

In summary, the present study comprehensively analyzed the pathways mediating radiosensitivity of PC cells and revealed the mechanisms through which radiosensitivity is determined. The adaptively expressed EGF may sensitize PC cells to radiation therapy through induction of the cyclin D1/P53/PARP signaling pathway, and IL-6/IGF-1 may contribute to the radioresistance of PC cells through coordinately activating the Stat3 and NF- κ B pathways. These findings are novel, and comparable to the reported pathways involved in the radioresistance in cancer stem cells, including the PI3K/Akt/mammalian target of rapamycin, extracellular signal-regulated kinase, glycolysis, vascular endothelial growth factor, autophagy, non-homologous end joining and homologous recombination DNA repair pathways (55). Furthermore, the present study has for the first time integrated these pathways to delineate the distinct signaling between the radiosensitive and radioresistant cancer cells.

Acknowledgements

Not applicable.

Funding

The present study was supported by grants from the Science and Technology Committee of Shanghai Municipality (grant no. 114119a7400 to YB); the National Natural Science Foundation of China (grant nos. 81372188 and 81672713 to JG, and 81402287 to LL); the State Key Laboratory of Oncogenes and Related Genes in China (grant no. 901406 to JG); the Special Fund for Innovation and Development of Science and Technology and Cultivation Fund for Major Projects and Innovative Team (grant no. 13X190030003 to JG); Shanghai Cancer Institute, China; the University Doctorate Research Fund for Freshly Recruited Teachers (grant no. 20130073120010 to LL); Ministry of National Education, China; the SJTU Interdisciplinary Research Grant (grant no. YG2015MS56 to LL).

Availability of data and materials

The datasets used and/or analyzed during the present study are available from the corresponding author on reasonable request.

Authors' contributions

XL performed experiments and drafted the manuscript. YH and HC performed the statistical analysis. XM, MY and RH contrib-

uted reagents/methods/analysis tools. HC and LX participated in irradiation of cells. BH, ML and LL helped prepare the figures. JG and YB designed the experiments. All the authors have read and approved the final version of the manuscript.

Ethics approval and consent to participate

Not applicable.

Patient consent for publication

Not applicable.

Competing interests

The authors declare that they have no competing interests.

References

1. Siegel RL, Miller KD and Jemal A: Cancer statistics, 2018. *CA Cancer J Clin* 68: 7-30, 2018.
2. Neoptolemos JP, Kleeff J, Michl P, Costello E, Greenhalf W and Palmer DH: Therapeutic developments in pancreatic cancer: Current and future perspectives. *Nat Rev Gastroenterol Hepatol* 15: 333-348, 2018.
3. Yogeve O, Barker K, Sikka A, Almeida GS, Hallsworth A, Smith LM, Jamin Y, Ruddell R, Koers A, Webber HT, *et al*: p53 loss in MYC-driven neuroblastoma leads to metabolic adaptations supporting radioresistance. *Cancer Res* 76: 3025-3035, 2016.
4. Maier P, Hartmann L, Wenz F and Herskind C: Cellular pathways in response to ionizing radiation and their targetability for tumor radiosensitization. *Int J Mol Sci* 17: 102, 2016.
5. Ziegler V, Henninger C, Simiontonakis I, Buchholzer M, Ahmadian MR, Budach W and Fritz G: Rho inhibition by lovastatin affects apoptosis and DSB repair of primary human lung cells *in vitro* and lung tissue *in vivo* following fractionated irradiation. *Cell Death Dis* 8: e2978, 2017.
6. Kashiwagi H, Shiraishi K, Sakaguchi K, Nakahama T and Kodama S: Repair kinetics of DNA double-strand breaks and incidence of apoptosis in mouse neural stem/progenitor cells and their differentiated neurons exposed to ionizing radiation. *J Radiat Res (Tokyo)* 59: 261-271, 2018.
7. Adams JM and Cory S: The BCL-2 arbiters of apoptosis and their growing role as cancer targets. *Cell Death Differ* 25: 27-36, 2018.
8. Tamm I, Wang Y, Sausville E, Scudiero DA, Vigna N, Oltersdorf T and Reed JC: IAP-family protein survivin inhibits caspase activity and apoptosis induced by Fas (CD95), Bax, caspases, and anticancer drugs. *Cancer Res* 58: 5315-5320, 1998.
9. Sochalska M, Tuzlak S, Egle A and Villunger A: Lessons from gain- and loss-of-function models of pro-survival Bcl2 family proteins: Implications for targeted therapy. *FEBS J* 282: 834-849, 2015.
10. Mirakhor Samani S, Ezazi Bojnordi T, Zarghampour M, Merat S and Fouladi DF: Expression of p53, Bcl-2 and Bax in endometrial carcinoma, endometrial hyperplasia and normal endometrium: a histopathological study. *J Obstet Gynaecol*: 1-6, 2018.
11. Murley JS, Miller RC, Weichselbaum RR and Grdina DJ: TP53 mutational status and ROS effect the expression of the survivin-associated radio-adaptive response. *Radiat Res* 188: 579-590, 2017.
12. Parida PK, Mahata B, Santra A, Chakraborty S, Ghosh Z, Raha S, Misra AK, Biswas K and Jana K: Inhibition of cancer progression by a novel trans-stilbene derivative through disruption of microtubule dynamics, driving G2/M arrest, and p53-dependent apoptosis. *Cell Death Dis* 9: 448, 2018.
13. Balart J, Pueyo G, de Llobet LI, Baro M, Sole X, Marin S, Casanovas O, Mesia R and Capella G: The use of caspase inhibitors in pulsed-field gel electrophoresis may improve the estimation of radiation-induced DNA repair and apoptosis. *Radiat Oncol* 6: 6, 2011.
14. Venturutti L, Romero LV, Urtreger AJ, Chervo MF, Cordo Russo RI, Mercogliano MF, Inurrigarro G, Pereyra MG, Proietti CJ, Izzo F, *et al*: Stat3 regulates ErbB-2 expression and co-opts ErbB-2 nuclear function to induce miR-21 expression, PDCD4 downregulation and breast cancer metastasis. *Oncogene*, 2015.

15. Braun DA, Fribourg M and Sealfon SC: Cytokine response is determined by duration of receptor and signal transducers and activators of transcription 3 (STAT3) activation. *J Biol Chem* 288: 2986-2993, 2013.
16. Arora R, Yates C, Gary BD, McClellan S, Tan M, Xi Y, Reed E, Piazza GA, Owen LB and Dean-Colomb W: Panepoxydione targets NF- κ B and FOXM1 to inhibit proliferation, induce apoptosis and reverse epithelial to mesenchymal transition in breast cancer. *PLoS One* 9: e98370, 2014.
17. Zeng Z, Sun Z, Huang M, Zhang W, Liu J, Chen L, Chen F, Zhou Y, Lin J, Huang F, *et al*: Nitrostyrene derivatives act as RXR α ligands to inhibit TNF α activation of NF- κ B. *Cancer Res* 75: 2049-2060, 2015.
18. Huang X, Lv B, Zhang S, Dai Q, Chen BB and Meng LN: Effects of radix curcumae-derived diterpenoid C on *Helicobacter pylori*-induced inflammation and nuclear factor kappa B signal pathways. *World J Gastroenterol* 19: 5085-5093, 2013.
19. Baens M, Bonsignore L, Somers R, Vanderheydt C, Weeks SD, Gunnarsson J, Nilsson E, Roth RG, Thome M and Marynen P: MALT1 auto-proteolysis is essential for NF- κ B-dependent gene transcription in activated lymphocytes. *PLoS One* 9: e103774, 2014.
20. Nakano K and Vousden KH: PUMA, a novel proapoptotic gene, is induced by p53. *Mol Cell* 7: 683-694, 2001.
21. Ren D, Tu HC, Kim H, Wang GX, Bean GR, Takeuchi O, Jeffers JR, Zambetti GP, Hsieh JJ and Cheng EH: BID, BIM, and PUMA are essential for activation of the BAX- and BAK-dependent cell death program. *Science* 330: 1390-1393, 2010.
22. Bryant HE, Schultz N, Thomas HD, Parker KM, Flower D, Lopez E, Kyle S, Meuth M, Curtin NJ and Helleday T: Specific killing of BRCA2-deficient tumours with inhibitors of poly(ADP-ribose) polymerase. *Nature* 434: 913-917, 2005.
23. Cook PJ, Ju BG, Telese F, Wang X, Glass CK and Rosenfeld MG: Tyrosine dephosphorylation of H2AX modulates apoptosis and survival decisions. *Nature* 458: 591-596, 2009.
24. Chande A, Prasad V, Jagtap JC, Shukla R and Shastry PR: Upregulation of survivin in G2/M cells and inhibition of caspase 9 activity enhances resistance in staurosporine-induced apoptosis. *Neoplasia* 6: 29-40, 2004.
25. Pardo FS, Su M and Borek C: Cyclin D1 induced apoptosis maintains the integrity of the G1/S checkpoint following ionizing radiation irradiation. *Somat Cell Mol Genet* 22: 135-144, 1996.
26. Borowiec A-S, Hague F, Gouilleux-Gruart V, Lassoued K and Ouadid-Ahidouch H: Regulation of IGF-1-dependent cyclin D1 and E expression by hEag1 channels in MCF-7 cells: The critical role of hEag1 channels in G1 phase progression. *Biochim Biophys Acta* 1813: 723-730, 2011.
27. Botto S, Streblow DN, DeFilippis V, White L, Kreklywich CN, Smith PP and Caposio P: IL-6 in human cytomegalovirus secretome promotes angiogenesis and survival of endothelial cells through the stimulation of survivin. *Blood* 117: 352-361, 2011.
28. Hov H, Våtsveen TK, Waage A, Sundan A and Borset M: Induction of Cyclin D1 by HGF, IGF-1 and IL-6 in a human myeloma cell line with a t(11;14). *Translocation. Blood* 108: 5055, 2006.
29. Ravitz MJ, Yan S, Dolce C, Kinniburgh AJ and Wenner CE: Differential regulation of p27 and cyclin D1 by TGF- β and EGF in C3H 10T1/2 mouse fibroblasts. *J Cell Physiol* 168: 510-520, 1996.
30. Vaira V, Lee CW, Goel HL, Bosari S, Languino LR and Altieri DC: Regulation of survivin expression by IGF-1/mTOR signaling. *Oncogene* 26: 2678-2684, 2007.
31. Wang H, Gambosova K, Cooper ZA, Holloway MP, Kassai A, Izquierdo D, Cleveland K, Boney CM and Altura RA: EGF regulates survivin stability through the Raf-1/ERK pathway in insulin-secreting pancreatic β -cells. *BMC Mol Biol* 11: 66, 2010.
32. Chi HC, Tsai CY, Tsai MM, Yeh CT and Lin KH: Roles of long noncoding RNAs in recurrence and metastasis of radiotherapy-resistant cancer stem cells. *Int J Mol Sci* 18: 18, 2017.
33. Hage-Sleiman R, Bahmad H, Kobeissy H, Dakdouk Z, Kobeissy F and Dbaibo G: Genomic alterations during p53-dependent apoptosis induced by γ -irradiation of Molt-4 leukemia cells. *PLoS One* 12: e0190221, 2017.
34. Deng WW, Hu Q, Liu ZR, Chen QH, Wang WX, Zhang HG, Zhang Q, Huang YL and Zhang XK: KDM4B promotes DNA damage response via STAT3 signaling and is a target of CREB in colorectal cancer cells. *Mol Cell Biochem* 449: 81-90, 2018.
35. Chishti AA, Baumstark-Khan C, Koch K, Kolanus W, Feles S, Konda B, Azhar A, Spitta LF, Henschenmacher B, Diegeler S, *et al*: Linear energy transfer modulates radiation-induced NF- κ B activation and expression of its downstream target genes. *Radiat Res* 189: 354-370, 2018.
36. Ménissier de Murcia J, Ricoul M, Tartier L, Niedergang C, Huber A, Dantzer F, Schreiber V, Amé JC, Dierich A, LeMeur M, *et al*: Functional interaction between PARP-1 and PARP-2 in chromosome stability and embryonic development in mouse. *EMBO J* 22: 2255-2263, 2003.
37. Lee SL, Ryu H, Son AR, Seo B, Kim J, Jung SY, Song JY, Hwang SG and Ahn J: TGF- β and hypoxia/reoxygenation promote radioresistance of A549 lung cancer cells through activation of Nrf2 and EGFR. *Oxid Med Cell Longev* 2016: 6823471, 2016.
38. Tang J, Guo F, Du Y, Liu X, Qin Q, Liu X, Yin T, Jiang L and Wang Y: Continuous exposure of non-small cell lung cancer cells with wild-type EGFR to an inhibitor of EGFR tyrosine kinase induces chemoresistance by activating STAT3. *Int J Oncol* 46: 2083-2095, 2015.
39. Diluvio G, Del Gaudio F, Giuli MV, Franciosa G, Giuliani E, Palermo R, Besharat ZM, Pignataro MG, Vacca A, d'Amati G, *et al*: NOTCH3 inactivation increases triple negative breast cancer sensitivity to gefitinib by promoting EGFR tyrosine dephosphorylation and its intracellular arrest. *Oncogenesis* 7: 42, 2018.
40. Li C, Iida M, Dunn EF, Ghia AJ and Wheeler DL: Nuclear EGFR contributes to acquired resistance to cetuximab. *Oncogene* 28: 3801-3813, 2009.
41. Wang YN, Lee HH, Lee HJ, Du Y, Yamaguchi H and Hung MC: Membrane-bound trafficking regulates nuclear transport of integral epidermal growth factor receptor (EGFR) and ErbB-2. *J Biol Chem* 287: 16869-16879, 2012.
42. Tong D, Ortega J, Kim C, Huang J, Gu L and Li GM: Arsenic inhibits DNA mismatch repair by promoting EGFR expression and PCNA phosphorylation. *J Biol Chem* 290: 14536-14541, 2015.
43. Hanada N, Lo HW, Day CP, Pan Y, Nakajima Y and Hung MC: Co-regulation of B-Myb expression by E2F1 and EGF receptor. *Mol Carcinog* 45: 10-17, 2006.
44. Lo HW, Hsu SC, Ali-Seyed M, Gunduz M, Xia W, Wei Y, Bartholomeusz G, Shih JY and Hung MC: Nuclear interaction of EGFR and STAT3 in the activation of the iNOS/NO pathway. *Cancer Cell* 7: 575-589, 2005.
45. Lo HW and Hung MC: Nuclear EGFR signalling network in cancers: Linking EGFR pathway to cell cycle progression, nitric oxide pathway and patient survival. *Br J Cancer* 94: 184-188, 2006.
46. Li SJ, Liang XY, Li HJ, Li W, Zhou L, Chen HQ, Ye SG, Yu DH and Cui JW: Low-dose irradiation promotes proliferation of the human breast cancer MDA-MB-231 cells through accumulation of mutant P53. *Int J Oncol* 50: 290-296, 2017.
47. Sumrejkanchanakij P, Tamamori-Adachi M, Matsunaga Y, Eto K and Ikeda MA: Role of cyclin D1 cytoplasmic sequestration in the survival of postmitotic neurons. *Oncogene* 22: 8723-8730, 2003.
48. Ahmed KM, Fan M, Nantajit D, Cao N and Li JJ: Cyclin D1 in low-dose radiation-induced adaptive resistance. *Oncogene* 27: 6738-6748, 2008.
49. Sheng L, Wan B, Feng P, Sun J, Rigo F, Bennett CF, Akerman M, Krainer AR and Hua Y: Downregulation of Survivin contributes to cell-cycle arrest during postnatal cardiac development in a severe spinal muscular atrophy mouse model. *Hum Mol Genet* 27: 486-498, 2018.
50. Tamari Y, Kashino G and Mori H: Acquisition of radioresistance by IL-6 treatment is caused by suppression of oxidative stress derived from mitochondria after γ -irradiation. *J Radiat Res (Tokyo)* 58: 412-420, 2017.
51. Yang HY, Qu RM, Lin XS, Liu TX, Sun QQ, Yang C, Li XH, Lu W, Hu XF, Dai JX, *et al*: IGF-1 from adipose-derived mesenchymal stem cells promotes radioresistance of breast cancer cells. *Asian Pac J Cancer Prev* 15: 10115-10119, 2014.
52. Yang N, Han F, Cui H, Huang J, Wang T, Zhou Y and Zhou J: Matrine suppresses proliferation and induces apoptosis in human cholangiocarcinoma cells through suppression of JAK2/STAT3 signaling. *Pharmacol Rep* 67: 388-393, 2015.
53. Iliopoulos D, Hirsch HA and Struhl K: An epigenetic switch involving NF- κ B, Lin28, Let-7 MicroRNA, and IL6 links inflammation to cell transformation. *Cell* 139: 693-706, 2009.
54. Ma J, Sawai H, Matsuo Y, Ochi N, Yasuda A, Takahashi H, Wakasugi T, Funahashi H, Sato M and Takeyama H: IGF-1 mediates PTEN suppression and enhances cell invasion and proliferation via activation of the IGF-1/PI3K/Akt signaling pathway in pancreatic cancer cells. *J Surg Res* 160: 90-101, 2010.
55. Chang L, Graham P, Hao J, Ni J, Deng J, Bucci J, Malouf D, Gillatt D and Li Y: Cancer stem cells and signaling pathways in radioresistance. *Oncotarget* 7: 11002-11017, 2016.